論文 12-3-25

인공수근관절과 의수를 개발하기 위한 최적설계법과 유한요소법에 의한 수근관절의 역학적해석

Force Analysis of Wrist Joint to Develop Wrist Implant and Mechanical Hand Using Optimization Technique and Finite Element Method

한 정 수*
Jung-Soo Han

(1997년 3월 14일 접수, 1997년 9월 20일 채택)

ABSTRACT

Many mathematical techniques have been developed to determine the muscle forces and force distribution in biomechanical human model, because it is so important to understand internal forces resisting external loading. However, a three-dimensional mathematical model of wrist joint, which is essential to develop solid modeling and artificial wrist joint, has not been well developed. This study proposed to define three-dimensional mathematical model of distal radius and ulna of the human wrist and to develop a detailed two-dimensional finite element through comparisons to existing analytical models and experimental tests.

This mathematical model were accurately recreated, allowing the internal tendon force as well as force transmission and distribution through the distal radius and ulna during dynamic loadings. The results found in this study indicate and support the findings of other investigator that cyclic loading condition results in higher compression force on distal radius and ulna and may be source of wrist disorder.

국 문 초 록

외력의 작용에 의해 발생되는 인체 내부의 내응력에 대한 이해가 중요하게 됨에 따라, 인간의 생체모델에서 근력이나 관절내에서의 응력분포를 밝히기 위한 다수의 수학적 모델이 소개 되어져 왔다. 그러나 고

* 한성대학교 산업시스템공학부 안전과학기술연구소

체모델이나 인공손목관절의 개발에 무엇보다도 중요한 실제에 가까운 3차원적인 수학적 모델의 개발은 지금까지 성공적이지 못하였다. 본 연구에서는 인체의 손목관절에서 원위 요골과 척골로 구성되어진 3차원 수학적 모델과, 정교하게 재구성되어진 2차원의 유한요소법을 이용한 수학적 모델을 완성함에 있다. 본 연구에서는 동적운동시의 손목관절에서 근력과 원위 요골과 척골로 전달 되어지는 힘과 관절내의 응력분포를 수학적 모델을 통하여, 정확하게 예측할 수 있는 가능성을 보여 주었다. 본 연구에서 추출되어진 결과는 동적운동 시 (반복운동), 손목관절을 이루고 있는 원위 요골과 척골에 상당히 많은 양의 힘이 전달되어짐을 밝히었으며, 이것은 반복운동에 의하여 손목관절에 종종 발생하는 누적성질환과 깊은 연계성을 갖고 있음을 보여 주고 있다.

1. INTRODUCTION

Hand and wrist injuries are very much common of general athletic and musician injuries. In spite of wrist pain and injury being a common affliction, its exact precipitating mechanism still eludes clinicians and researchers alike. Epidemiological studies have shown that mechanical factors play a significant role in the onset of these symptoms. One such factor is the exposure of the wrist to repetitive work. The methods used to determine the force in the wrist were a rigid body spring model[1~5], pressure sensitive film[6,7], and strain gages[8,9]. Several other studies[9~11] applied the load cell to radius and ulna directly. The internal mechanics of the human wrist are poorly understood due to the complexity of its small irregular bones and connecting ligament structures. Detailed information is not known about the stress distribution within carpal bones, contact pressures between bones or carpal displacement and ligament and forces when the carpus is loaded.

In this study, a three-dimensional nonlinear optimization based model[12] was formulated to predict forces in the tendon and force transmitted through the distal radius and ulna of wrist during dynamic loading and to develop a detailed two-dimensional finite element through comparisons to existing analytical models and experimental tests.

2. METHOD AND MATERIALS

2.1 A Three-dimensional Nonlinear Optimization Model

A total of three mathematical models (23, 10, and 6 tendons model) were formulated to predict tendon force as well as the compressive force on distal radius and ulna. 23 tendons model consists of all of tendons crossing the wrist including 6 prime wrist motors, 4 thumb motors, and 13 extrinsic finger motors. However, 6 tendons model recruited prime wrist mover motors only (ECRL, ECRB, ECU, FCR, FCU, and APL). 10 tendons model includes EPL, FPL, APL, EPB along with 6 prime wrist mover motors. The formulation of a mathematical model to predict forces in the force transmitting structures spanning a wrist joint requires the following data : (a) lines of action of the structures and their points of application with respect to global axis system, (b) physiological areas of cross-section of the tendon, and (c) their permissible intensities. The point of application point (moment arm) and cross-sectional areas of tendon were obtained from previous studies[5].

The wrist external loading conditon (flexion and extension moment) required to move the wrist can be obtained using Lagrangian dynamics model, since the wrist torque is related to the wrist position . The required wrist trajectories with function of time t were $60°\cos(2\pi t)$ for flexion-extension and $-20°\sin(2\pi t)$ for radial-ulnar deviation during for 1 second. The Lagrangian dynamic model used in this study is the following; $T=H(\theta)\ddot{\theta}+N(\theta, \dot{\theta})$ where H : inertia moment matrix, N : torque vector due to Coriolis and centripedal acceleration, friction, and gravity[13].

⟨Mathematical Model⟩

Using the above data set, the six equilibrium equations and a set of constraints were formulated by considering the free body diagram of the distal radius and ulna.

$M_x = m_i Z_i F_i - T_x = 0$
$M_y = (l_i Z_i n_i X_i) F_i = 0$
$M_z = m_i X_i F_i + T_z = 0$
$F_x = l_i F_i + F_{urx} = 0$
$F_y = m_i F_i + F_{ury} = 0$
$F_z = n_i F_i + F_{urz} = 0$
$F_i > = 0$
$F_i / A_i - S_i < = 0$

where F_i-force in the ith tendon; l_i, m_i, n_i-the direction cosines of the ith tendon; X_i, Z_i-coordinates of the centroid of the ith tendon; S_i-maximun intensity of the ith tendon; A_i-cross-sectional areas of ith tendon; T_x, T_z-external flexion/extension and radial/ulna moments; and F_{urx}, F_{ury}, F_{urz}-force contributions of distal radius and ulna. The problem was indeterminate and a solution was sought using a nonlinear optimization algorithm. The function $\{(F_i/A_i - S_i)^3\}^{1/3}$ was minimized to find an optimum solution[12].

2.2 A Two-dimensional Finite Element Model

A simple FEM consisting of the radius(r), ulna (u), scaphiod(s), lunate(l), capitate(c) and triangular fibrocartilage complex (TFCC) was constructed of the wrist in the neutral position. This simple model is composed of 4573 4-node plane-stress linear quadrilateral elements, 24 tension-only spring elements and 143 slideline interface elements generated using the ABAQUS finite element software package(HKS, Pawtucket, R. I.).

Once the simple model was completed and analyzed, a more complex FEM of the wrist in the natural position, consisting of the radious, ulna, scaphoid, lunate, capitate, triquetrum(tq), hamate (h), trapezoid(tz), second through fifth metacarpals(mc) and triangular fibrocartilage complex (TFCC), was generated. This complex model is composed of 8538 4-node plane-stress linear quadrilateral elements, 175 tension-only spring elements and 280 slideline interface elements also using ABAQUS.

The proximal ends of the radius and ulna were rigidly fixed in both models. The distal edge of the capitate in the simple model and distal edges of the metacarpals in the complex model were fixed against radial-ulnar deviation. The medial and lateral slides of the capitate were constrained by slideline elements which acted as through the hamate and trapezoid were still present and the distal edge of the TFCC was restrained in the proximal-distal direction to represent the missing triquetrum in the simple model. In the complex model, the radial edge of the trapezoid was fixed against radial-ulnar deviation(modeling as if the trapezoid carpal bone and the first metacarpal, which overlap the trapezoid in the natural position, were still present).

Loading conditions used in this study for both models were the following : The capitate was loaded with a 100N distributed load across its distal edge in the simple model. The netacarpals were load in complex model, as if the hand were grasping with a force of 1kg, along their mid-axes with compressive loads of : 33.0N second metacarpal, 42.2N third metacarpal, 25.6N and 19.7N fourth and fifth metacarpals as reported by Horii, et al (1990).

The FEM material properties (cortical bone : Young's Modulus (E)=17.0 Gpa, possion's ratio (V)=0.31; cancellous bone : E=1.5 GPa, v=0.25; articular cartilage : E=11.5 GPa, v=0.40; TFCC : E=23.0 MPa, v=0.40) and ligament stiffnesses (ranging between 40-350N/mm) were based on values reported in literature[14~17]. Frictionless interface were assumed between articular surfaces. The Young's Modulus for TFCC is presently unknown. We estimated the modulus to be double that of cartilage since the TFCC is a composition of cartilage and ligaments.

3. RESULTS

In the Opitimization based model, the profile of distal radius/ulna compression and tendon forces during flexion/extension and radial/ulnar deviation were shown in Fig. 1~Fig. 4. The maximum forces transmitted through radius and ulna during dynamic loading were listed in Table 1.

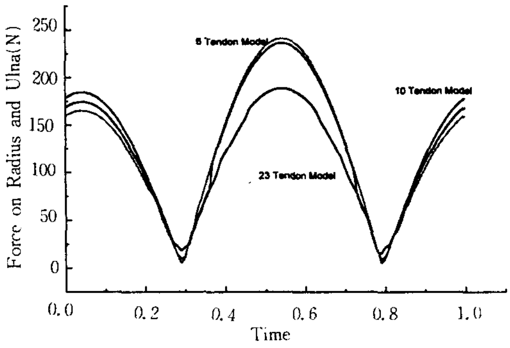

Fig. 1 Compressive Force Transmitted Through Radius During Dynamic Flexion/Extension Motion

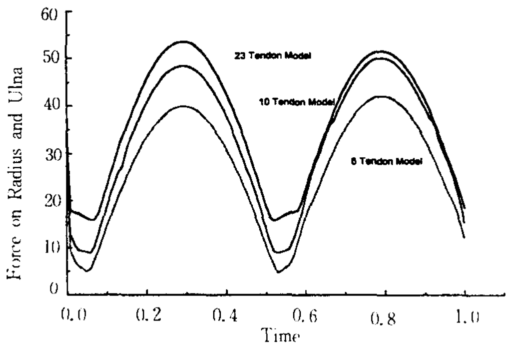

Fig. 2 Compressive Force Transmitted Through Radius During Dynamic Radial/Ulnar Deviation Motion

Table 1 The Maximum Forces Transmitted through radius and Ulna during Dynamic Loading with Three Different Models

Model	Maximun Force (N)			
No. Tendon	Flexion	Extension	Radial Dev.	Ulnar Dev.
23	174	188	53	51
10	184	236	48	50
6	164	241	39	42
Mean	174	222	47	47

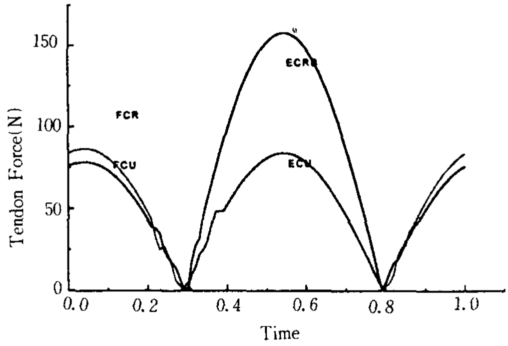

Fig. 3 Tendon Force Required During Dynamic Flexion/Extension Motion

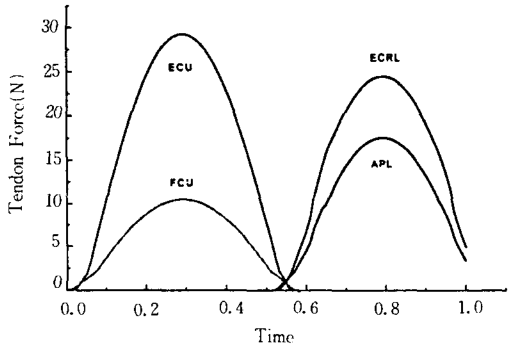

Fig. 4 Tendon Force Required During Dynamic Radial/Ulnar Deviation Motion

Regardless of the number of tendon formulated in the mathematical model, the greater force on radius and ulna was found during extension rather than flexion. The extension mode induced distal radius and ulna compression that was about 27% higher than the flexion mode. However, during radial/ulnar deviation, there was no much difference between compression forces. During the cyclic flexion/extension loading, either ECU and ECRB or FCR and FCU play a important role in resisting the external load. However, for radial/ulnar deviation, greater forces were required from a combination of either ECU and FCU or APL and ECRL, respectively.

In the finite element method based model, a noticeable shifting of the carpal bones downward towards the ulna was observed. This shifting is

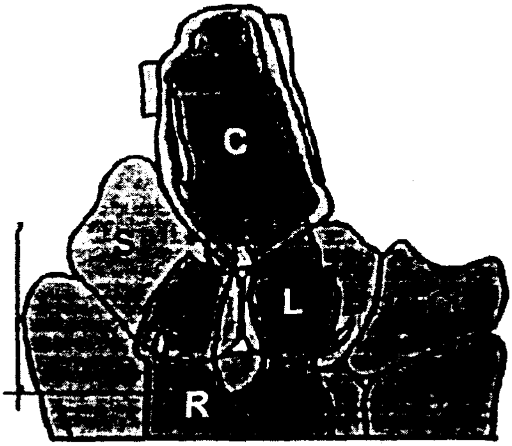

Fig. 5 Stress Distribution/Contours in Simple FEM Model

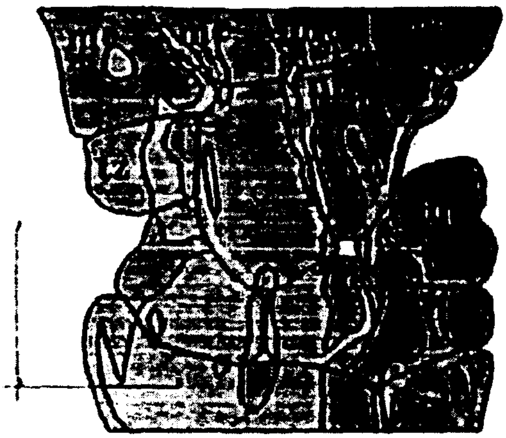

Fig. 6 Stress Distribution/Contours in Complex FEM Model

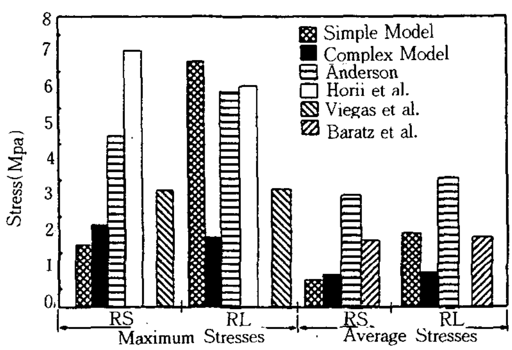

Fig. 7 Comparison of Average Contact Stresses with Other Studies

expected with compressive loading of the carpus[16). Stress-contours of both models show concentrations of stresses through the capitate and down into the scaphoid and lunate(Fig. 5~Fig. 6). This finding was expected because the majority of carpal fractures occur in these bones[17). Maximum contact stresses were comparable to those reported by other researchers[3,18,19). Average contact stresses were comparable to previous reports[3,18,20)(Fig. 7). The ratio-lunate ligament experienced a tensile force of 29.45N in the simple model and 1.83N in the complex model. The scapho-triquetral ligament experienced no tensile force in the simple model (Fig. 5) but, a 0.79N tensile force in the complex model(Fig. 6). The complex model compares more favorably than the simple model with other reported results[16,18). The differences between the simple and complex models are most likely due to loading and boundary condition which were not present in other reported analytical and experimental models. The percentage of axial load distribution across the radius (77.0%) and ulna (23.0%) corresponded to that of work performed by Palmer and Werner[21).

4. CONCLUSION

This results indicate and support the findings of other investigator that cyclic loading condition results in higher compression force on distal radius and ulna and may be source of wrist disorder.

Simple and complex two-dimensional finite element models of the wrist joint were developed and verified with previously published work. This study is being continued to include experimental vertification. Once the two-dimensional models are vertified experimentally, the knowledge gained can be applied to more complex and accurate three-dimensional finite element wrist model.

This work was funded by grants from Korea Research Foundation (본 연구는 학술진흥재단 연구지원금으로 수행되었음).

REFERENCES

1) H. Tsumura, S. Himeno, T. Kojima, M. Kido "Biomechanical Analysis of Kienbock's Disease" Seikeigeka, pp. 1399~1402, 1982.
2) K.N. An, S. Himeno, H. Tsumura, T. Kawai, E.Y.S. Chao "Pressure Distribution on Articular Surface : Application to Joint Stability Evaluation", J. Biomechanical Eng., Vol. 23, pp. 1013~1020, 1990.
3) E. Horii, M. Garcia-Elias, K.N. An, A.T. Bishop, W.P. Cooney, R.L. Linscheid, E. Y.S. Chao, "Effect on Force Transmission Across the Carpus in Procedures Used to Treat Kienbock's Disease", J. Hand Surgery, Vol. 15, pp. 393~400, 1990.
4) H. Tsumura, S. Himeno, K.N. An, W.P. Cooney, E.Y.S. Chao, "Biomechanical Analysis of Kienbock's Disease", Transaction of the Ortjopedic Society, p. 208, 1987.
5) H. Tsumura, S. Himenos, "Load Transmission and Injury of the Wrist Joint", Biomechanics Symposium, Vol. 56, pp. 5~8, 1983.
6) E. Horii, K.N. An, E.Y.S. Chao, "Force Distribution across the Wrsit Joint Using a Pressure Transducer", Wrist Biomechanics Workshop, Mayo Clinic, October, 1990.
7) W.H. Short, F.W. Werner, M.D. Fortino, A.K. Palmer, "Distribution of Pressures and Forces on the Wrist after Simulated Intercarpal Fusions and Kienbock's Disease", Wrist Biomechanics Workshop, Mayo Clinic, October, 1990.
8) A.K. Palmer, F.W. Werner, "Biomechanics of the Distal Radioulnar Joint", Clinical Orthopedic, Vol. 187, pp. 26~35, 1984.
9) F.W. Werner, R.R. Glisson, D. Murphy, A.K. Palmer, "Force transmission Through the Distal Radioulnar Carpal Joint : Effect of Ulnar Lenthening and Shortening", Handchirurgie, Vol. 18, pp. 304~308, 1986.
10) T.E. Trumble, R.R. Glisson, A.V. Seaber, J.R. Urbanick, "Forearm Force transmission after Surgiical Treatment of Distal Radioulnar Joint Disorders", J. Hand surgery, Vol. 12, pp. 196~202, 1987.
11) R.M. Patterson, P. Todd, S.F. Viegas, P. McCarty, "Forearm Load Distribution", Ninth Annual Conference on Biomedical Wngineering Research, Houston, Texas, pp. 7~8, 1991.
12) J.S. Han, and V.K. Goel, "A Nonlinear Optimization Force Model of the Human Lumbar Spine", International J. Ergonomics, Vol. 5, pp. 125~132.
13) R. Colbaugh, K. Glass, and J. Ryu, "Adaptive Control of a Human Wrist Motion Simulator", Internatinal J. of Modeling and Simulation, Vol. 11, pp. 93~103, 1991.
14) S.C. Cowin, Bone Mechanics, CRC Press, Boca Raton, FL, 1989.
15) H. Huber-Betzer, T.D. Brown, C. Matteck, "Some effects of Global Joint Morphology on Local Stress Aberrations Near Imprecisely Reduced Intra-Articular Fractures", J. Biomechanics, Vol. 23, pp. 811~822, 1990.
16) M.A.R. Freeman, Adults Articular Cartilage, Ch 6., 1979.
17) S.F. Viegas, A.F. Tencer, J. Cantrell, M. Chang, P. Clegg, C. Hicks, C. O'Meara, J.B. Williamson, "Load Transfer Characteristics of the Wrist, Part Ⅰ. The Normal Joint", J. Hand Surgery, Vol. 12A, pp. 971~978, 1987.
18) D. Anderson, "A Finite Element Analysis of the Radiocarpal Joint", Conference Proceedings of the 17th Annual Meeting of the American Society of Biomechanics, p. 69, 1993.
19) S.F. Viegas, A.F. Tencer, J. Cantrell, M. Chang, P. Clegg, C. Hicks, C. O'Meara, J.B. Williamson, "Load Transfer Characteristics of the Wrist, Part Ⅱ. Perilunate Instability", J. Hand Surgery, Vol. 12A,

pp. 978~985, 1987.
20) M. E. Baratz, J. D. Des Jardins, D. D. Anderson, J. E. Imbriglia, "Displaced Fractures of the Distal Radius : The Effect of Joint Surface Incongruities on Intra-Articular Contact stresses", Proceedings of the 39th Annual Meeting of the orthopedic Research Society, p. 106, 1993.
21) A. K. Palmer, F. W. Werner, "Biomechanics of the Distal Radioulnar joint", Clinical Orthopedics, Vol. 187, pp. 26~35, 1984.